SPEED CONTROL OF MARINE DIESEL ENGINES- A PARAMETRIC ANALYSIS

S. Youssef, M. Hanafi and M. Morsy
Department of Marine Engineering and Naval Architecture, Faculty of Engineering, Alexandria University, Alexandria, Egypt.

ABSTRACT

The dynamics of naturally aspirated marine Diesel engines with proportional plus derivative speed regulator are analyzed in a parametric study for mathematical simulation. Varying operating parameters involve mean piston speed, brake mean effective pressure, volumetric efficiency and excess air factor. The state space model is derived too for investigating the controllability of the plant and to tackle the stability problem by a backward algorithm for Lyapunov function generation. Dynamic behavior of the plant alone, open and closed loops, in time and frequency domains are portrayed and specifications of each domain are argued with each selected operating condition.

NOMENCLATURE

[A]	System matrix		
$A/F)_{c.c}$	Chemically correct air-fuel ratio.		
a	Level arm of Centrifugal weights (cm)		
a_1	Cross sectional area of power piston (cm^2)		
a_2	Cross sectional area of receiving piston (cm^2)		
a_3	Cross sectional area of responding piston (cm^2)		
[B]	Control vector.		
b	Lever arm of centrifugal weights (cm).		
bmp	Brake mean effective pressure (Pa)		
C_1	$=\dot{m}_o/u_o$	(kg/s% rack stroke).	
C_2	$=\dot{m}_o/\omega_{e,o}$	(kg).	
C_3	$=p_{e,o}/\dot{m}_o$	(Joule/kg).	
C_4	$=\eta_{tr}.\eta_p/I\omega_{e,o}$	($s/kg.m^2$).	
C_5	$=1/I\omega_{e,o}$	($s/kg.m^2$).	
C_6	$=3\eta_{tr}.\eta_p.P_{eo}/\omega_{e,o}$	(Joule).	
C_f	$=2\ (2\pi\ C_g/60)^2$		
C_g	Gear ratio between engine and governor.		
C_p	Specific heat at constant pressure of air (K Joule/Kg.°K).		
C_r	b/a		
C_v	Specific heat at constant volume of air (K Joule/Kg.°K).		
CV	Calorific value of fuel (KJ/Kg).		
C_nH_m	Hydrocarbon fuel (for Cetane:n =16,m=34).		
d	Bore of engine cylinders (m).		
db	Decibel = 20 $\log_{10}$ (Magnitude).		
d_p	Diameter of plunger of fuel pump (m).		
e	Displacement of pilot value (mm).		
F_c	Centrifugal force on governor balls (N).		
F_s	Spring force on governor (N).		
G(s)	Forward path transfer function.		
$G_1(s)$	Transfer function of the plant.		
$G_2(s)$	Transfer function of controller.		
G_m	Gain margin.		
g	gravitational acceleration (m/s^2)		
H(s)	Transfer function of feedback elements.		
h	Displacement of power piston (mm).		
I	Mass polar moment of inertia of rotating parts including added mass of water ($Kg.m^2$)		
$\bar{[I]}$	Unity matrix.		
j	$=\sqrt{-1}$		
k	Reaction scale of pilot value due to hydraulic flow (N/mm)		
$\bar{k}$	Fuel pump constant= $\rho_f \frac{\pi}{4}.d_p^2.I_p.\frac{1}{2\pi}$ (kg/cycle)		
k_2	$=\partial z/\partial n_i\,|_o$	(cm/rpm)	
k_3	$=C_f\ C_r\ M\ n_o^2$	(N/cm).	

k_4 $=2\ C_f\ C_r\ M\ R_o\ n_o$ (N/rpm).
k_d Gain of derivative action of speed governor (s).
k_1 Propeller power constant $(W/(rad/s)^3)$.
k_p Gain of proportional action of speed governor.
k_s Spring constant of the centrifugal governor (N/cm).
k_{s1} Spring constant of feedback piston (N/mm).
[L] Output row vector.
l Stroke of engine pistons (m).
l_1 Sleeve lever arm (cm).
l_2 Sleeve lever arm (cm).
l_p Stroke of plunger of fuel pump (m)
M Mass of one of the centrifugal balls (kg).
M_p Percentage maximum overshoot.
M_r Resonant peak (db).
m Multiplicity of the i^{th} residue.
m_1 Number of residues of n(s).
$\dot{m}_f$ Rate of fuel injected into the cylinder (kg/s).
$\dot{m}_j$ Rate of fuel delivered by fuel pump(kg/s).
$\dot{m}_o$ Nominal value of $\dot{m}_f$ (kg/s).
mps Mean piston speed (m/s).
N number of cylinders of Diesel engine.
n Rate of revolutions of the Diesel engine. (rpm).
n_i Desired speed from Diesel engine (command signal) (rpm).
o Suffix indicating the nominal value.
[P] Positive definite matrix to generate Lyapunov's function.
p_m Phase margin (degrees).
P Oil pressure under feedback piston (Pa).
P_e Brake power (w)
P_f Friction power lost in shaft bearings (w).
P_1 Power absorbed by the propeller (w).
q Pilot valve flow $(mm^3/s.mm)$.
q_1 Needle valve flow $(mm^3/s.Pa)$.
R Radius of rotation of flyballs (cm).
r Dummy variable.
s Laplace operator (s^{-1}).
s_i i^{th} residue of n(s).
$[...]^T$ Transpose of a matrix.
t Time (s).
u Fuel rack position (%)
V Scalar Lyapunov function
[X] State variable vector.
x Displacement of the bottom spring plate (mm).
y Displacement of responding piston (mm).
y_o Maximum stroke of fuel rack (cm).
z Displacement of upper spring plate (reference signal) (mm).
α Angle of inclination of arms of centrifugal balls (degrees)
α_c crank shaft angle.
$\Delta...$ Change in...
ε_1 Levers ratio.
ε_2 Levers ratio.
η_{bth} Brake thermal efficiency of Diesel engine
η_m Mechanical efficiency of Diesel engine.
η_p Propeller efficiency behind ship.
$\eta_{p.o.w}$ Propeller efficiency in open water.
η_{rr} Relative rotative efficiency.
η_{tr} Transmission efficiency of propulsion shaft.
η_{vol} Volumetric efficiency of Diesel engine.
λ Excess air factor of Diesel engine.
ρ Density of combustion air in Diesel engine (kg/m^3).
ρ_f Density of fuel (kg/m^3).
τ Delay time constant in controller (s).
τ_c Delay time of fuel (s).
τ_d Transportation lag of fuel (s).
$\psi(\sigma_1,\sigma_2,\sigma_3)$ Any function of σ_1, σ_2 and σ_3
ω Frequency of input/output (rad/s).
ω_1 Gain cross-over frequency (rad/s).
ω_c Angular speed of Diesel engine (rad/s).
ω_π Phase cross-over frequency Rad/s)

INTRODUCTION

The evolution of control theories since the oldest Watt type governor adopted for speed regulation of the earliest steam engines, beside the continual progressive innovations in memorable topics. In various control teritories has been demonstrated at length in a previous work [1,2].

Moreover, the groundwork of speed regulation of Diesel engines varying from simplified treatments of profound modelling and sophisticated simulations has been illustrated too in [1,2]. The contributions of Raven, Engja, Garvey, Solodovnikov, Welbourn,

Wozniak, Barrett, Andersen, Topfer, Rudert, Thompson, Woodward, Latorre, Smith, Ford, Krutov, Kyrtatos and Koumbarelis [1,2] have appreciably enriched the scientific literature concerned with the industrial speed regulation of Diesel engines. The establishment of conventional controllers, namely proportional, integral derivative actions and possible combinations, dates back to the few past decades; the matter which urged contemporary researches to develop new control algorithms in engineering technology whose merits overweigh those of traditional regulators. Analysis and discussion of such developed techniques namely, Pseudo derivative feedback (PDF), Proportional minus delay (PMD) controls, Parameter-optimized and optimal control have been demonstrated in [3,4].

It has become now rule of thump that the plant dynamics particularly, the time delays and transportation lags which incorporates together with the nature of the external perturbation-whether being deterministic or stochastic to which the plant is subjected, determine the principles of adequate choice of traditional controllers.

It is also well-known that if the control designer prerequisites do not imply the absence of steady-state error, the proportional plus derivative controller with the inevitable contained time delays, becomes the most appropriate selection to meet excessive dynamic hehavior of a plant. Merits of introducing derivative action are expressed in its instantaneous interference improving the automatic control loop performance.

The larger the time delays or dead time built in the plant, the larger should be the gain of the derivative action controller. In addition the study of the influence of both conventional and non-conventional controllers on the speed regulation of naturally aspirated marine Diesel' engines has been tackeled in [3,4], or part load dynamic performance of the marine supercharged Diesel propulsion plant with state feedback regulator was presented in [1,2], in an integrated and sophisticated thermodynamic model for slow speed marine Diesel engines.

The objective of this research work is to adopt a reduced and simplified mathematical description for a directly-coupled naturally aspirated marine Diesel engine with proportional-derivative speed regulator for the analysis of the dynamic behavior of the automatic loop in control domains.

The Diesel engine is assumed to operate at varying working conditions represented in changes in fuel rack index rotational speed, excess air factor and volumetric efficiency with the consequent resulting changes in the rate of injected fuel brake power, brake specific fuel consumption and brake mean effective pressure. Transient and frequency responses displayed represent those of the plant alone and those of the feedback system to the command signal; absolute and relative stability analyses are not ignored.

This work represents an extraction of an integrated research.

MODELING OF THE MARINE DIESEL ENGINE

Simulation of the Diesel engine was dealt with in details in [3,5], however the model is reproduced briefly for convenience.

Taylor linearizing formula is used namely:

$$\psi_{(\sigma 1,\ \sigma 2,\sigma 3)} - \psi_{(\sigma 1,0,\ \sigma 2,0,\sigma 3,0,0)} = \Delta\Psi =$$

$$= \sum_{r=1}^{\infty} \left(\frac{\partial \psi}{\partial \sigma_1} \Big|_o \Delta\sigma_1 + \frac{\partial \psi}{\partial \sigma_2} \Big|_o \Delta\sigma_2 + \frac{\partial \psi}{\partial \sigma_3} \Big|_o \Delta\sigma_3 \right)^r \quad (1)$$

For dead time, pade approximations are used namely:

$$e^{-\tau_d s} \simeq \left(1 - \frac{\tau_d}{2r}\right) / \left(1 + \frac{\tau_d}{2r}.s\right)]^r \quad (2)$$

It is to be noted that the first term only in equations (1) and (2) will be used.

The fuel pump analysis produces:

$$\left.\begin{aligned} \dot{m}_j &= \bar{k}.\omega_e.u \\ \dot{m}_f &= \frac{e^{-\tau_d.s}}{1+\tau_c.s}\dot{m}_j \end{aligned}\right\} \quad (3)$$

The brake power and the power absorbed by the propeller can be written as:

$$\left.\begin{aligned} P_e &= 1000^{*}\eta_m.\eta_{bth}cv.\dot{m}_f \\ P_1 &= k_1.\omega_e^3 \end{aligned}\right\} \quad (4)$$

The dynamics of the propulsion shaft can be written from Largrange's or D' Alembert's equations which yield:

$$\left.\begin{aligned} &\frac{d}{dt}\left(\frac{1}{2}.I\omega_e^2\right)=P_e-P_f-P_1 \\ &\text{where : } P_f=p_e-\eta_{tr}.\eta_p.P_e \end{aligned}\right\} \quad (5)$$

The linearization of equations (3,4,5) results in:

$$\left.\begin{aligned} \Delta\dot{m}_f &= (C_1.\Delta u + C_2.\Delta\omega_e).\left(\frac{1-0.5^{*}\tau_d.s}{1+0.5^{*}\tau_d.s}\right).\left(\frac{1}{1+\tau_c.s}\right), \\ \Delta P_e &= C_3.\Delta\dot{m}_f, \\ \Delta\dot{\omega}_e &= C_4.\Delta P_e - C_5.\Delta P_1, \\ \Delta P_1 &= C_6.\Delta\omega_e, \\ \text{where } \tau_c &= \frac{\alpha_c}{\omega_e}, \\ \alpha_c &= \frac{2\pi}{N} \text{ and} \\ \tau_d &= \frac{\pi}{\omega_e.N} \end{aligned}\right\} \quad (6)$$

A proportional plus derivative controller is shown in Figure (1) whose simulation is included in [4,6] and is shortly reproduced for completion Neglecting gravitational and frictional forces it could be written:

$$\left.\begin{aligned} z &= k_2.n_i, \\ F_c &= 2^{*}\left(\frac{2\pi C_g}{60}\right)^2.M.R.n^2 = C_F.M.R.n^2, \\ 0.5F_c.b..\sin\alpha &= 0.5D_s.a.\sin\alpha, \\ \text{or: } F_s &= C_r.C_f.M.R.n^2 = \frac{k_s}{10}(z - x.\varepsilon_2 h) \\ \text{and } R &= -C_r x \end{aligned}\right\} \quad (7)$$

Linearization of equations (7) gives:

$$\left.\begin{aligned} \Delta z &= k_2 = \Delta n_i, \\ \Delta F_s &= k_3.\Delta R + k_4.\Delta n = \frac{k_s}{10}(\Delta z - \Delta x - \varepsilon_2.\Delta h) \end{aligned}\right\} \quad (8)$$

$$\text{or : } \Delta x = \left(\frac{k_s}{10}\Delta Z - \frac{k_s}{10}\varepsilon_2\Delta h - k_4\Delta n\right)/\left(\frac{k_s}{10} - C_r k_3\right) \quad (9)$$

To get force on the pilot valve, moments are taken about point O_2 (Figure (1);

$$\left[\frac{k_s}{10}(-\varepsilon_2\Delta h + \Delta z - \Delta x) - k_4.\Delta n\right](1+l_2) = k.\Delta e.l_2 \quad (10)$$

The displacement balance of the walking beam is:

$$\Delta e = (\Delta x.l_2 - \Delta y.\, l_1) / (l_1+l_2) \quad (11)$$

The balancing of the receiving and responding pistons can be determined from the continuity equation:

$$(a_2\,\epsilon_1\,\Delta h - a_3\,.\,\Delta\dot{y})\,10^4\Delta = q_1.\,\Delta P \quad (12)$$

Similarly, the continuity equation for the flow from the pilot valve to the power piston is:

$$q.\,\Delta e = a_1\,\Delta\dot{h}^{*}10^4 \quad (13)$$

The force balance on the walking beam can be written by taking moments about point O_1 (Figure 1), [6]:

$$k.\Delta e.\left(\frac{l_1}{l_1-l_2}\right) + \frac{a_3}{10^4}.\Delta P = k_{s1}\Delta y \quad (14)$$

Combining equations (3) to (6) inclusive, yields to block diagram of the marine Diesel engine plant which is shown in Figure (2). Identically, combining equations (9) to (14) inclusive, give the block diagram of the governor as obtained and indicated in Figure (3). Figure (4) joins both block diagram for the feedback speed control system.

A simplification of the $(PD)_2$ property speed governor is obtained by neglecting its second order delay, particularly, it is minute in magnitude. The automatic speed control loop with $(PD)_1$ governor is illustrated in Figure (5).

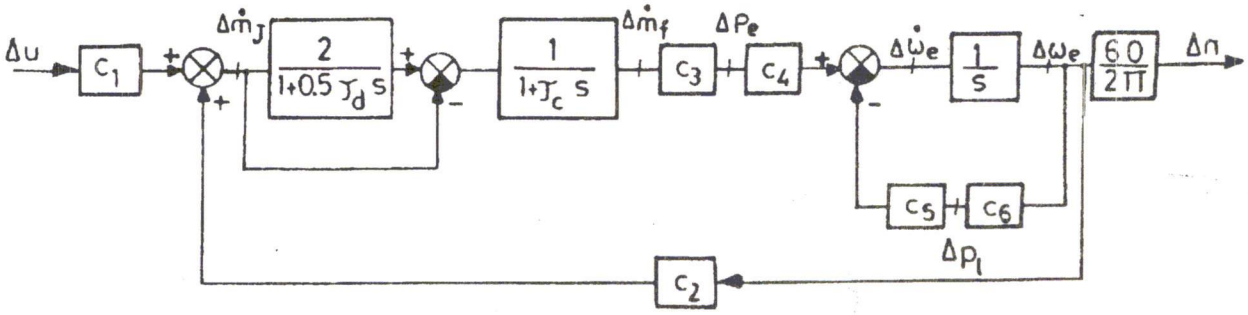

Figure 1. Block Diagram of Marine Diesel Engine.

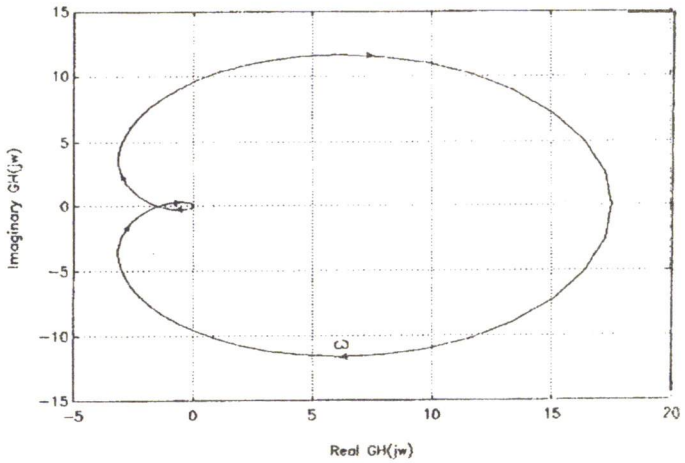

Figure 2. Unstable O.L. Nyquist Plot, with P1 Governor, Kp = 10, Kd = 0, Case 1.

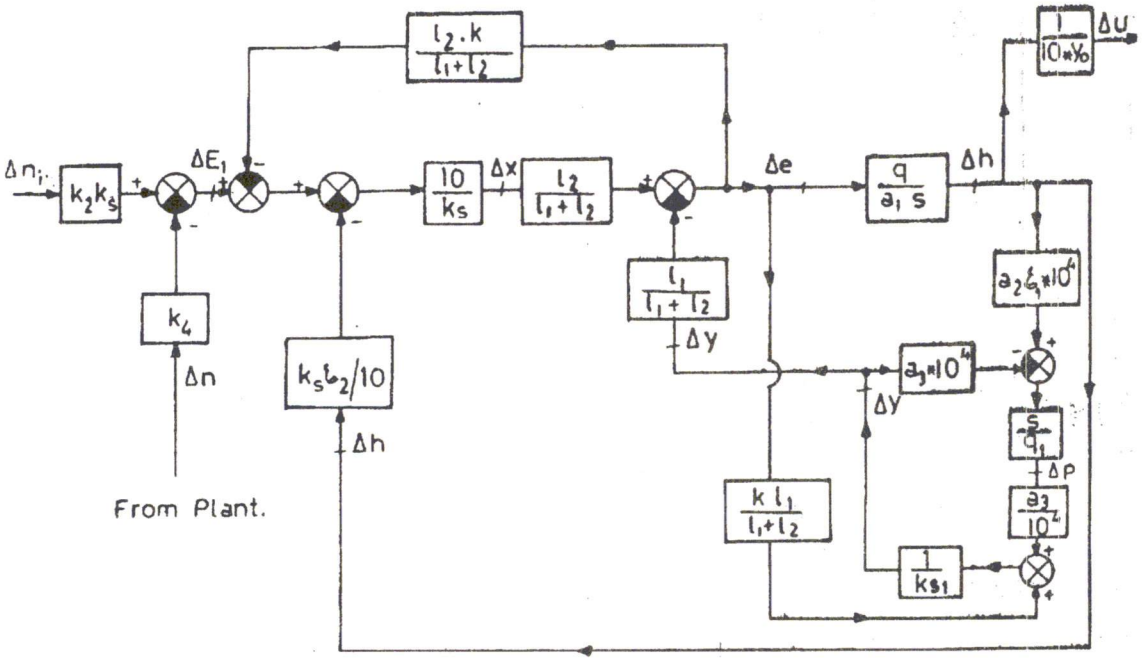

Figure 3. Block Diagram for Simulation of $(PD)_2$ Governor.

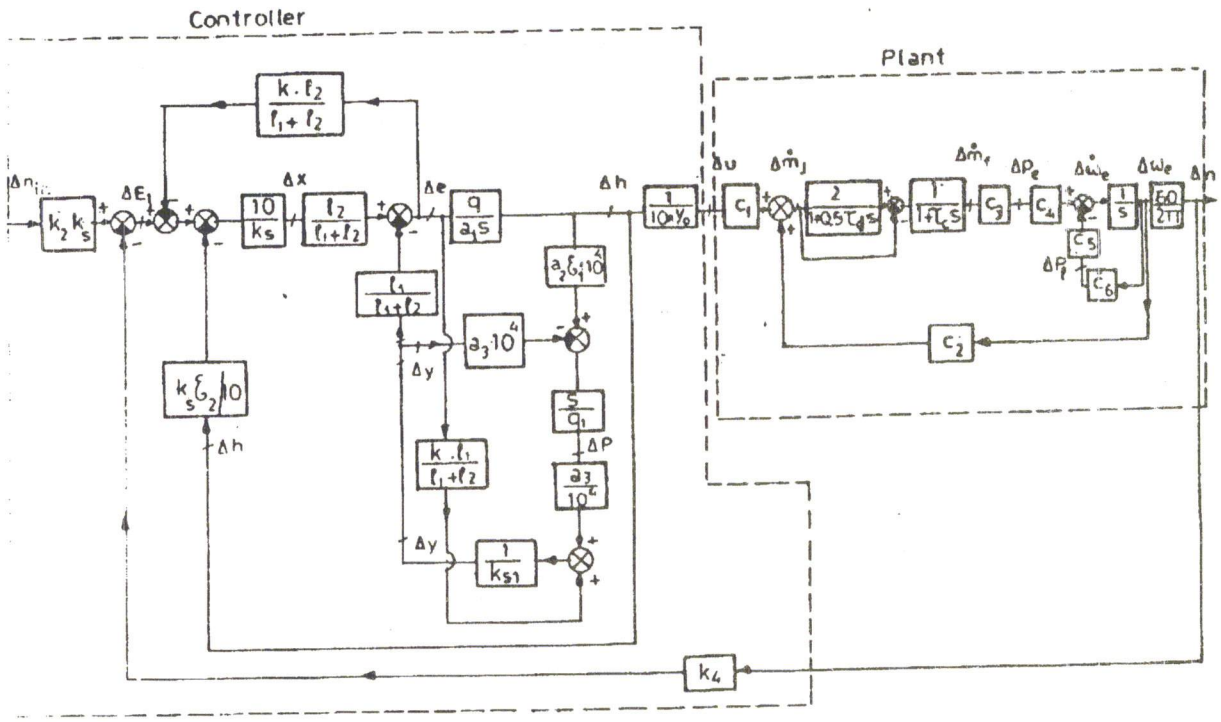

Figure 4. Block Diagram of Plant and Governor.

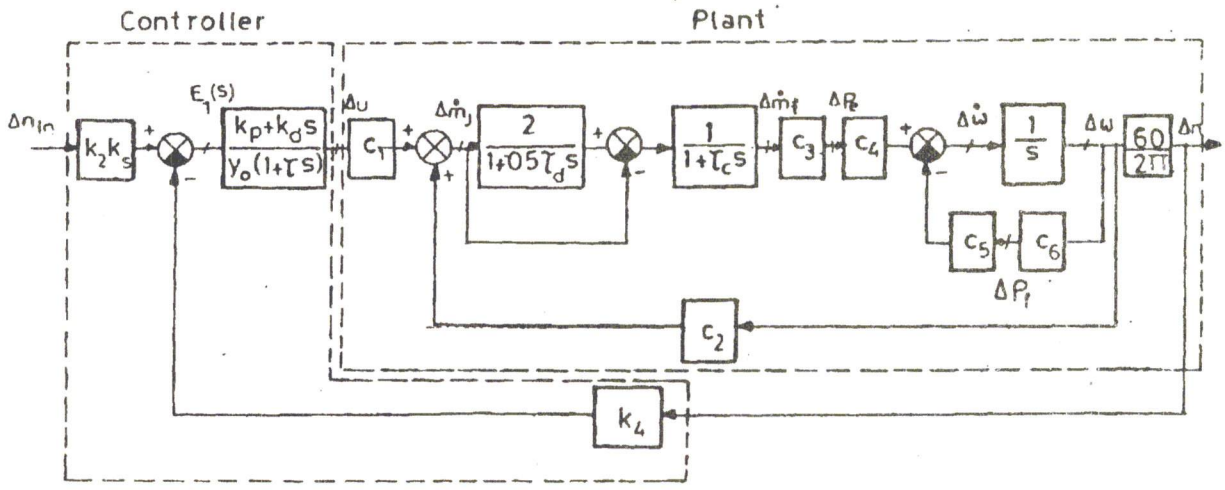

Figure 5. The Automatic Speed Control Loop with $(PD)_1$ Governor.

NUMERICAL DATA PROCESSED

A two stroke, six cylinders, naturally aspirated, marine Diesel engine is considered.
Particulars of the engine are as follows:

$d = 0.8$ (m), $1 = 1.8$ (m), $\frac{1}{d} = 2.25$, $\eta_m = 0.85$.

$\eta_{tr} = 0.98$, $\eta_p = \eta_{r.r}$, $\eta_{p.o.w} = 0.6$, bmp = 10(atm),

mps = 6 (m/s), $\lambda = 1.15$, $\eta_{vol} = 0.92$,

$u = 0.751$, $I = 84000$ (Kg.m^2),

fuel is Cetane (C_{16} H_{34}), CV = 41870 (kJ/kg)

The basic Steady-State operation equations are summarized below:

$$C_nH_m + (n+\frac{m}{4}))(O_2 + 3.76N_2) \xrightarrow{c.c} n\,CO_2 + \frac{m}{2}\,H_2O + 3.76\,(n+\frac{m}{4})N_2,,$$

$$A/F)_{c.c} = (n+\frac{m}{4}))\,(32 + 3.76^{*}\,28) / (12n+m) = 14.882,$$

$$\rho = 101.3/\,(1.005 - 0.718)^{*}\,293) = 1.19\ (kg/m^3),$$

$$\bar{k} = \dot{m}_o / (\omega_{c,o}.\ u_o) = 0.5797 / (2\,\pi\,(100) / 60)^{*}\,0.75),$$

= 0.0738 (kg /cycle), (engine (rpm) = 100 for (mps) = 6 (m/s)),

$$\dot{m}_f = \bar{k}.\ u.\ \omega_e,\ p_e = \dot{m}_f.\ (CV)\ \eta_{bth},$$

$$P_e = ((bmp).\ \frac{\pi}{4}.\ d^2.\ 1.N>n)/60 = 0.09045\ (bmp.\ n = \dot{m}_f.\ (CV).\ \eta_{bth},$$

$$\eta_{vol} = ((bsfc).\ P_e.\ A/F)_{c.c}\ \lambda) / \frac{\pi}{4}.d^2.I.N.n.\rho^{*}60^{*}1000)$$

$$= 0.3474^{*}\ 10^{-5\,*}\ ((bsfc).\ (bmp).\ \lambda),$$

$$\eta_{bth} = (P_e/1000)^{*}\ 3600/\ (P_e/1000)\ (CV).\ (bsfc).\ = 3600/\ (CV).\ (bsfc),$$

$\tau_c = 2\,\pi\,/\,(N.\omega_e)$ and $\tau_d = \pi\,/\,(N.\omega_e)$

For fuel density ρ_f = 880, stroke to diameter ratio plunger = 5,
Pinion to plunger diameter ratio = 2.25 then:
Helix rotation angle between extreme positions $2\pi/3$ corresponding to 1/3 Periphery, the maximum stroke of the fuel rack y_o can be computed as [3,4]:

$$y_o = \frac{2.25\,\pi}{3}\sqrt{\frac{60^{*}4}{5\,\pi}\,\frac{P_e}{N.n.\eta_{bth}.(CV).\rho_f}} = 6\,(cm)$$

The varying operating conditions chosen for the marine Diesel engine are namely: (bmp), (mps), λ and η_{vol}) together with the resulting particulars are shown in Table (1). Besides, the coefficients of the plant as control system are presented in Table (2), where case 1 is considered to be the reference case. In what concerns the centrifugal regulator, its selected parameters for the sake of stability, are as follows:

R_o = 6 (cm), M=0.3 (kg), C_r = b/a = 2, C_g =1

$C_f = 2(2\pi\ C_g/60)^2 = 0.0219,$

$k_4 = 2\ C_f.\ C_r.M.R_o.n_o = 0.15768$ for mps = 6 (m/s),

$k_4 = 0.18448$ for mps = 7 (m/s),

k_d = 4, k_d = 1 (s) and τ = 0.4 (s),

Based on computer results, the reference element ($k_2.k_s$) is selected as 0.18017115 (N/rpm) in order to eliminate the steady-state error for the reference case.

DIGITAL COMPUTATIONS

The reduction of the block diagram of the marine Diesel power plant indicated in Figure (2) yields:

$$G_1(s) = \frac{\Delta n(s)}{\Delta u(s)} =$$

$$\frac{-4.77465^{*}C_1C_3C_4\tau_d{*}s+9.55^{*}C_1C_3C_4}{0.5\tau_c\tau_d s^3+(0.5\tau_c\tau_d C_5C_6+\tau_c+0.5\tau_d)s^2+(C_5C_6(\tau_c+0.5\tau_d)+0.5\tau_d C_2C_3C_4+1)s+(C_5C_6-C_2C_3C_4)} \quad (15)$$

Table 1. Engine's varied parameters.

Case	bmp (atm)	mps (m/s)	λ	η_{vol}
1	10	6	1.15	0.92
2	10	6	1.15	0.95
3	10	6	1.35	0.92
4	10	6	1.35	0.95
5	10	7	1.15	0.92
6	10	7	1.15	0.95
7	10	7	1.35	0.92
8	10	7	1.35	0.95
9	12	6	1.15	0.92
10	12	6	1.15	0.95
11	12	6	1.35	0.92
12	12	6	1.35	0.95
13	12	7	1.15	0.92
14	12	7	1.15	0.95
15	12	7	1.35	0.92
16	12	7	1.35	0.95

Substituting for the values of the coefficients shown in Table (2) for case (1) and transforming the transfer function of equation (15) into state space form by Bush's direct programming [7] gives:

$$\left.\begin{aligned}[\dot{X}] &= [A][x] + [B] * \Delta u \\ \Delta n &= [L][X]\end{aligned}\right\} \qquad (16)$$

where

$$[A] = \begin{bmatrix} -1.6987 & 20.451 & -10.2253 \\ 0 & -40 & 40 \\ 0.554 & 0 & -10 \end{bmatrix},$$

$$[B] = \begin{bmatrix} 0 \\ 0 \\ 7.73 \end{bmatrix} \text{ and}$$

$$[L] = [9.55 \ 0 \ 0]$$

The controllability test matrix for the plant [8] is given by:

$$[[B] \quad [A][B] \quad [A]^2[B]] \qquad (17)$$

Whose value is:

$$= \begin{bmatrix} -0 & -79 & 7248 \\ 0 & 309 & -15460 \\ 7.73 & -77 & 729 \end{bmatrix}$$

and it's determinant equals $7.8779^{*}10^{6} \neq 0$, hence the plant is controllable.
Similarly, the observability test matrix of the plant [8] is given by:

$$[[L^T] \quad [A^T][L^T]^2 \quad [L^T]] \qquad (18)$$

Whose determinant's value is $9.1072^{*}\ 10^{6} \neq 0$, hence the plant is observable.. In fact, the plant is completely controllable and completely observable for the sixteen cases shown in Tables (1) and (2). As an illustration of the plant's dynamics, Figure (6) shows the unit step responses for cases (1) and (2).

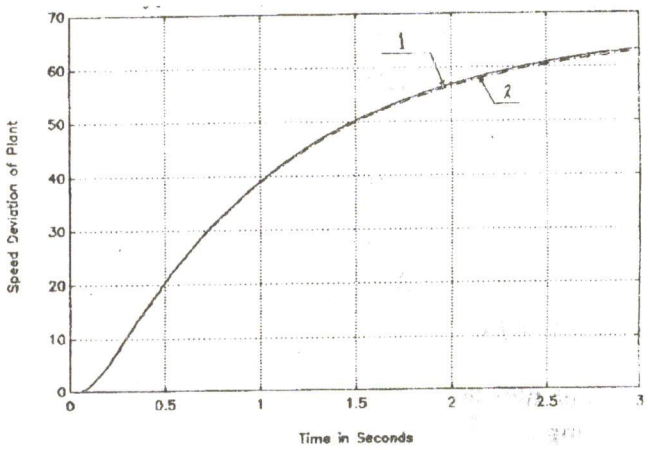

Figure 6. Tansient Response of Plant m.p.s.=6, λ=1.15, b.m.p.=10.

In regards to the absolute stability the closed loop system matrix for case (1) is:

$$[A] = \begin{bmatrix} 0 & 1 & 0 & 0 \\ 0 & 0 & 1 & 0 \\ 0 & 0 & 0 & 1 \\ -9058.2 & -3465.7 & -571 & -54.2 \end{bmatrix}$$

The Lyapunov's stability theorem [9,10] states that if there exists a differentiable function V representing the energy of the dynamic system in the neighborhood of the origin of the coordinate X_i, it satisfies the conditions that V is positive definite and V is negative semi-definite, then the point $X_i = 0$ is asymptotically stable-in the sense of Layapuov.

Table 2. Coefficients of plant as control system.

Case	C_1, $(\frac{\text{Kg/s}}{\text{\% rack stroke}})$	C_2 (kg)	$C_3^* 10^6$ Joule/kg)	$C^{4*} 10^6$ (S/kg.m^2)	$C_5^* 10^{-6}$ (S/kg.m^2)	$C_6^* 10^{-6}$ (Joule)	τ_c (sec)	τ_d (sec)
1	0.733	0.0554	15.2959	0.6685	1.137	1.494	0.1	0.05
2	0.7998	0.0573	14.7021	0.6685	1.137	1.494	0.1	0.05
3	0.6574	0.0471	17.984	0.6685	1.137	1.494	0.1	0.05
4	0.6782	0.0486	17.431	0.6685	1.137	1.494	0.1	0.05
5	0.902	0.0554	15.295	0.5726	0.9744	1.494	0.086	0.043
6	0.931	0.0572	14.812	0.5726	0.9744	1.494	0.086	0.043
7	0.7669	0.0471	17.4834	0.5726	0.9744	1.494	0.086	0.043
8	0.7912	0.0486	17.4316	0.5726	0.9744	1.494	0.086	0.05
9	0.7721	0.0553	18.375	0.6685	1.137	1.7924	0.1	0.05
10	0.7989	0.0572	17.7584	0.6685	1.137	1.7924	0.1	0.05
11	0.6574	0.0471	21.5826	0.6685	1.137	1.7924	0.1	0.05
12	0.681	0.0488	20.8347	0.6685	1.137	1.7924	0.1	0.05
13	0.901	0.0553	18.376	0.5726	0.9744	1.8252	0.086	0.043
14	0.832	0.0572	17.758	0.5726	0.9744	1.8252	0.086	0.043
15	0.7693	0.047	21.5127	0.5726	0.9744	1.8252	0.086	0.043
16	0.7939	0.0487	20.8479	0.5726	0.9744	1.8252	0.086	0.043

A technique to implement the backward procedure to generate a Laypunov's function for linear systems [11], is to impose the condition that V should be negative semi-definite or:

$$\dot{V} = [A]^T [P] + [P] [A] = [\bar{I}] \qquad (19)$$

Solution of equation (19) yields:

$$[P] = \begin{bmatrix} 0.3 & -0.5 & -2 & 0.5 \\ -0.5 & 2 & -0.5 & -39 \\ -2 & -0.5 & 39 & -0.5 \\ -0.5 & -39 & -0.5 & 21482 \end{bmatrix}$$

The positive definiteness of the matrix [P] is satisfied by Sylvester's theorm [7] if all sub determinants of [P] are positive. These values are 0.3, 0.35, 4.575 and 1371. 7, which ensures the exitence of a Lyapunov's function and the asymptotic stability of the closed loop system. Consequently,

$$V = [X_1\ X_2\ X_3\ X_4]\ [P]\ X_1\ X_2 X_3 X_4]^T \qquad (20)$$

Another pictorial technique applied in the frequency domain for investigating the absolute stability is the Mikhailov's criterion [7] which is displayed for cases (1) and (2) in Figures (7-a,7-b).

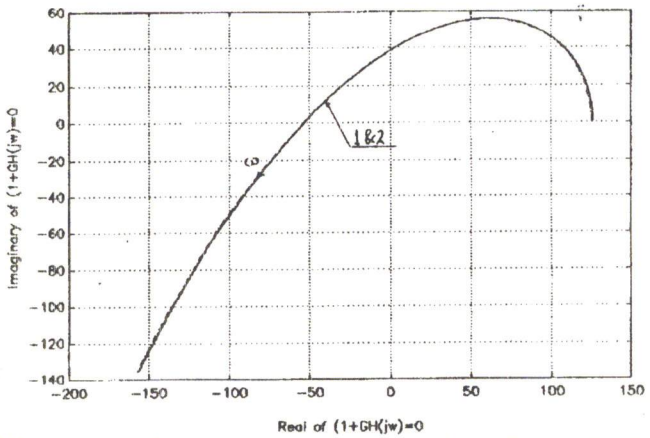

Figure 7a. Mikhailov's Stability Plot Cases 1&2, w=0:0.25:10.

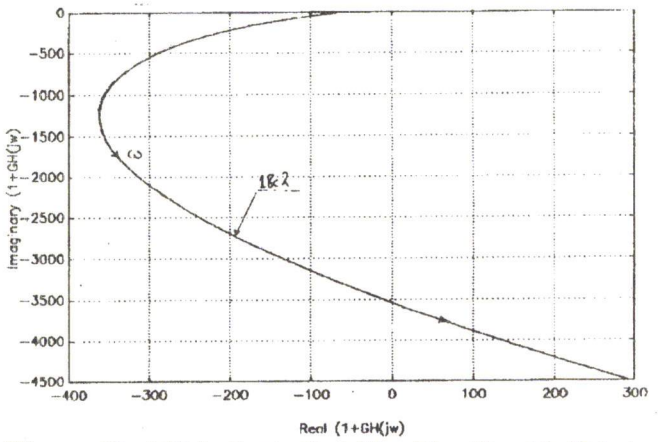

Figure 7b. Mikhailov's Stability Plot Kp=10, Kd=1s, w=8:0.4:25, Cases 1&2.

The plots start at the positive real axis, rotate in an anti-clockwise sense, intersecting quadrants in a sequential order and are terminated at the quadrant corresponding to the degree of the characteristic equation i.e. the fourth quadrant; a matter which guarantees the absolute stability of the closed loop. The stability problem investigation can be extended to all the sixteen cases of the plant with the $(PD)_1$ speed regulator. The transient response may be computed from Cauchy's theorem namely:

$$\Delta n(t) = \sum_{i=1}^{m} \frac{1}{(m-1)} \lim_{s \to si} \left\{ \frac{d^{m-1}}{ds^{m-1}} . \Delta n(s) . e^{st} . (s - s_i)^m \right\} \quad (21)$$

The transient response, open loop polar plots and closed loop Bode plots for cases (1) and (2) are demonstrated in Figure (8,9) and (10) respectively.

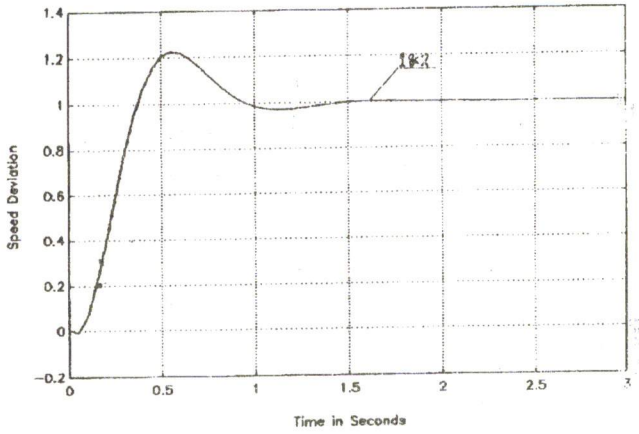

Figure 8. C.L. Transient Response: m.p.s.=6, λ=1.15, b.m.p.=10.

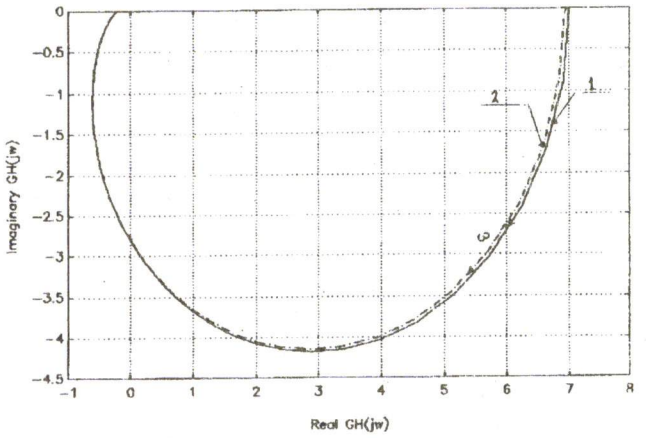

Figure 9. O.L Polar Plot b.m.p.=10, m.p.s=6, λ=1.15.

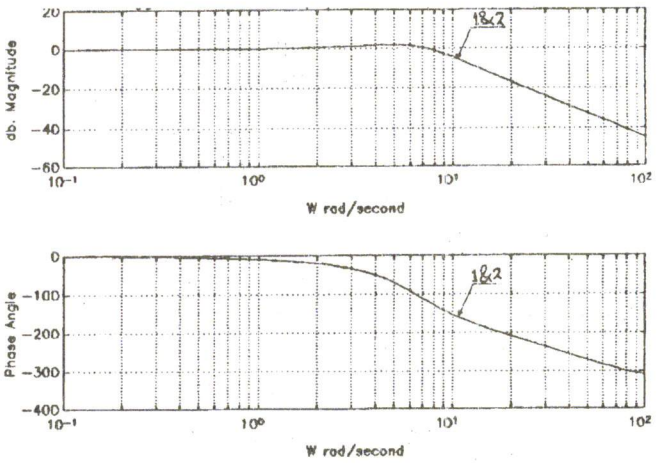

Figure 10. C.L. Bode Plots with $(PD)_1$ Governor Kp=4, Kd=1s, Cases 1&2.

As a comparison between cases (1,3), Figures (11,12,13) and (14) illustrate the transient responses of the plants only, the closed loop transient responses, the open loop and closed loop Bode plots respectively. In an identical manner, the transient responses of the plants, the closed loop transient responses, the open loop Nichols, the open loop Nyquist plots and the closed loop Bode plots for cases (1,5) are portrayed in Figures (15-19) inclusive. Concerning cases (1,9) comparisons including the transient responses of the plants, the closed loop transient responses, the open loop magnitude-phase plots, closed loop Bode plots and closed loop Nichols plots are displayed in Figures (20-23b) inclusive. Other comparisons for different case studies-with emphasis on the influence on mp and mps-in time domain analysis of closed loop and open loop polar plots are scanned in Figures (24-29) inclusive. Moreover, the relative stability measures namely the gain and phase margins the phase crossover and gain crossover frequencies (ω_π, ω_1) for cases (1 through 5,9 and 13) of the automatic speed control with $(PD)_1$ governor are tabulated in Table (3).

Table 3. Relative stability of the automatic loop at different operating conditions with $(PD)_1$ governor.

Case	G_m	P_m	ω_π	ω_1
1	4.6278	53.3851	13.5551	4.7185
2	4.6528	53.5733	13.5553	4.7012
3	4.6449	53.4227	13.5737	4.7169
5	4.4656	50.3931	15.4981	5.5253
9	4.1618	51.1539	14.1016	5.3197
13	3.8607	47.2276	15.7156	6.2595

$$G_2(s) = \frac{k_p + d_d.s}{y_o(1+\tau.s)}$$

kp = 4, kd=1 s, τ =0.4s and y_o = 6cm

This research has been executed in the computer laboratory at the department of marine engineering and naval architecture using the symbolic package DERIVE [12] and the numerical package oriented for the analysis and synthesis of control systems MATLAB 4.0 [13].

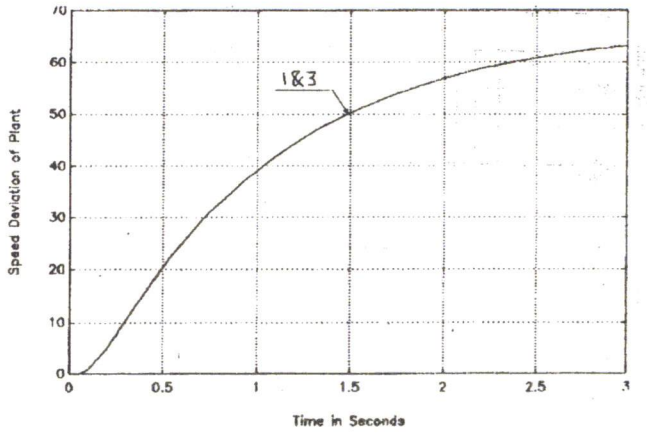

Figure 11. Transient Response of Plant m.p.s.=6, b.m.e.p.=10, η_{vol}=0.92.

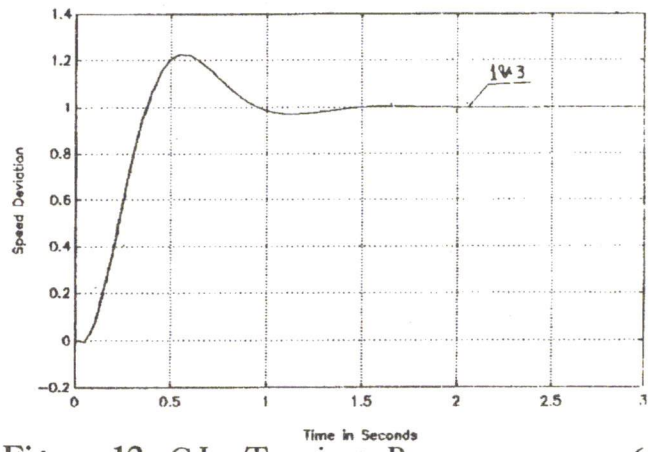

Figure 12. C.L. Transient Response m.p.s.=6, b.m.e.p.=10, η_{vol}=0.92.

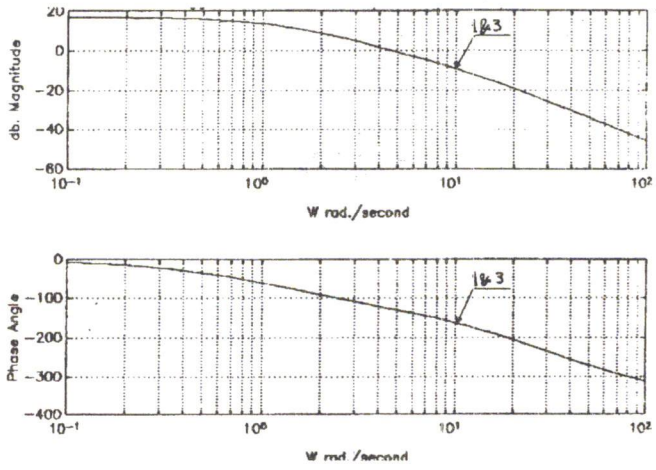

Figure 13. O.L. Bode Plots b.m.p.s.=10, m.p.s.=6, η_{vol}= 0.92.

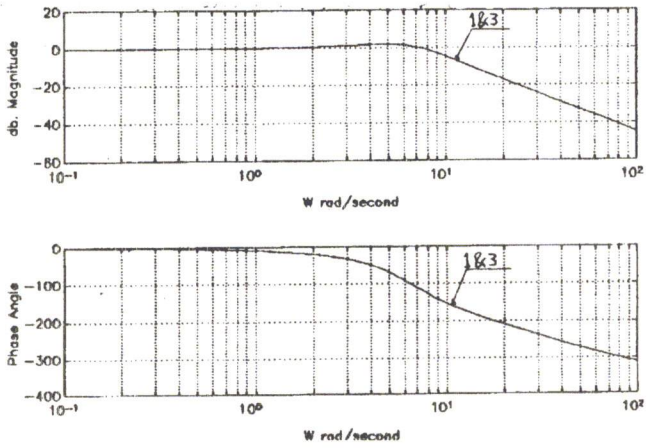

Figure 14. Bode plots with (PD) 1 governor k_p=4, k_d = 1s cases 1 & 3.

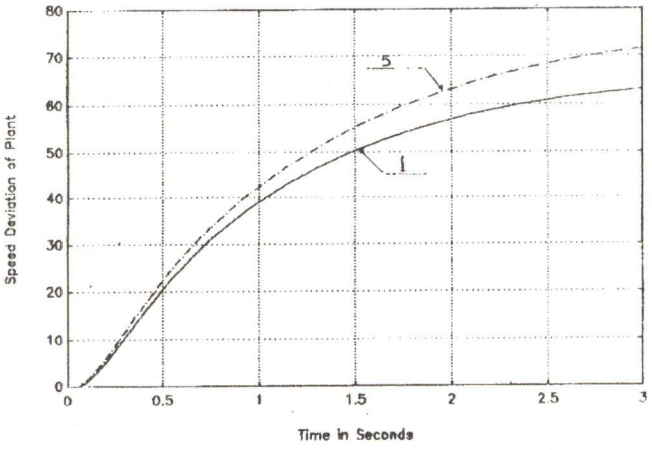

Figure 15. Transient response of plant b.m.e.p =10, λ =1.15, η_{vol}=0.92.

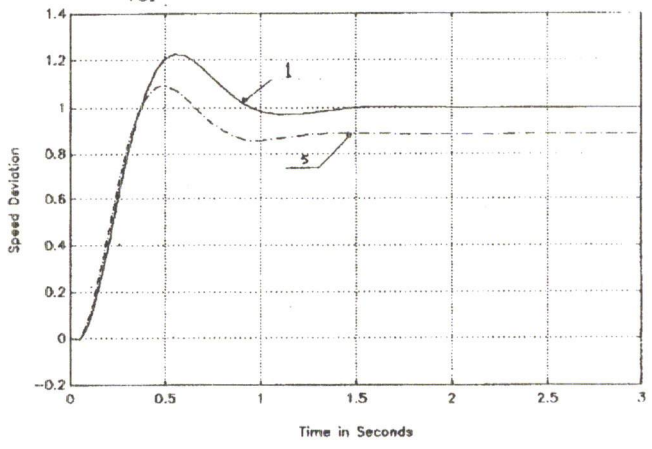

Figure 16. Transient response: b.m.e.p =10, λ =1.15, η_{vol}=0.92.

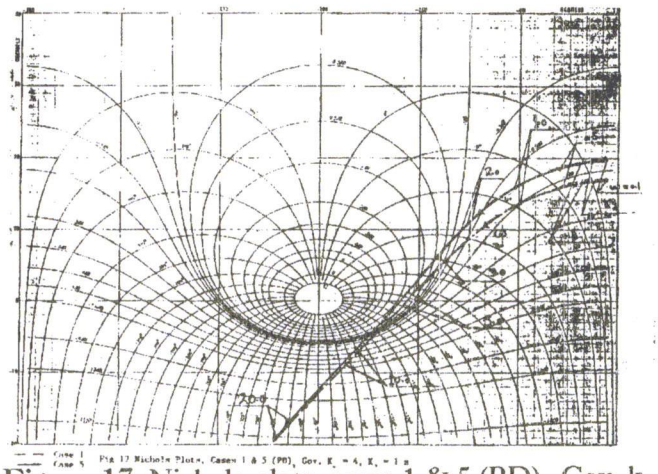

Figure 17. Nichols plots, cases 1 & 5 $(PD)_1$ Gov. k_p = 4, k_d = 1s.

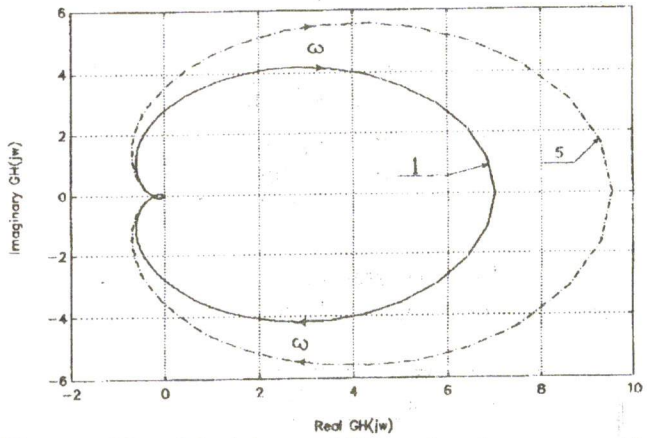

Figure 18a. Nyquist stability plot b.m.e.p. =10, λ=1.15, η_{vol}=0.92

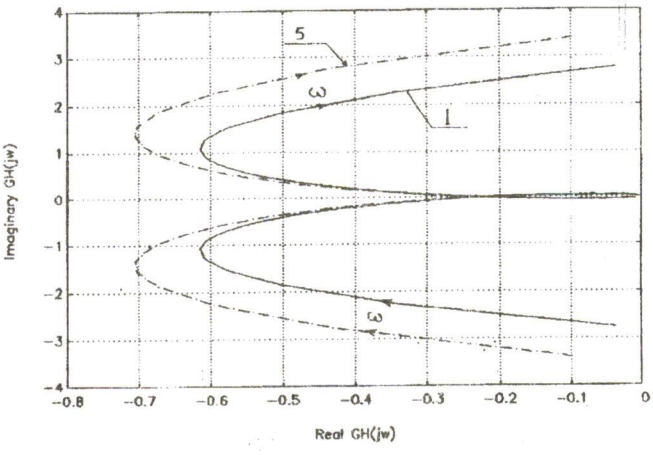

Figure 18b. O.L. end portion of Nyquist plot b.m.e.p. =10, λ=1.15, η_{vol}=0.92, ω=2:0.4:40.

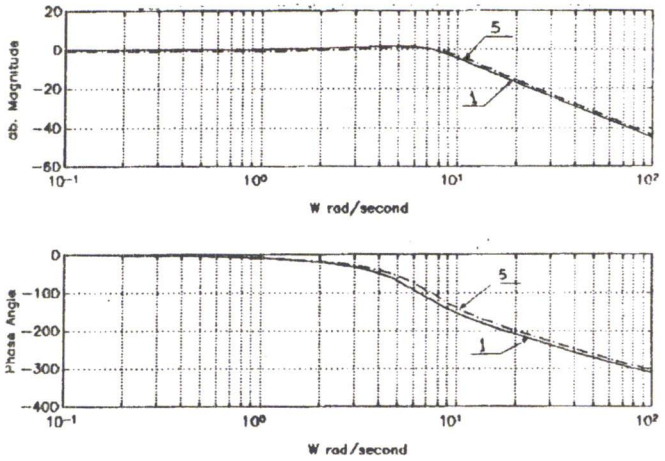

Figure 19. C.L. Bode plots with (PD) governor k_p=4,k_d=1s cases 1 & 5.

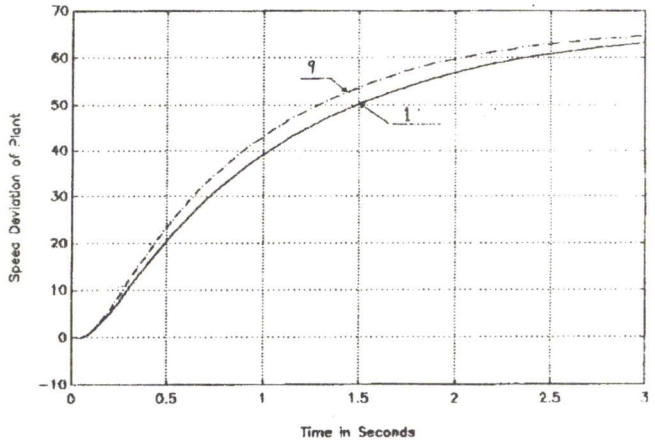

Figure 20. Transient response of plant m.p.s. = 6, λ=1.15, η_{vol}=0.92.

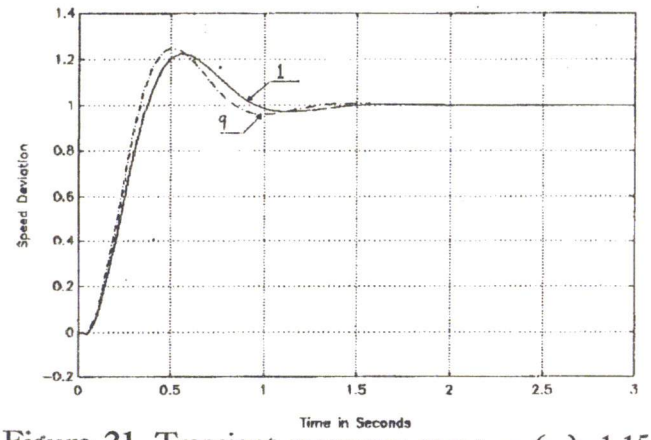

Figure 21. Transient response: m.p.s. = 6, λ=1.15, η_{vol}=0.92.

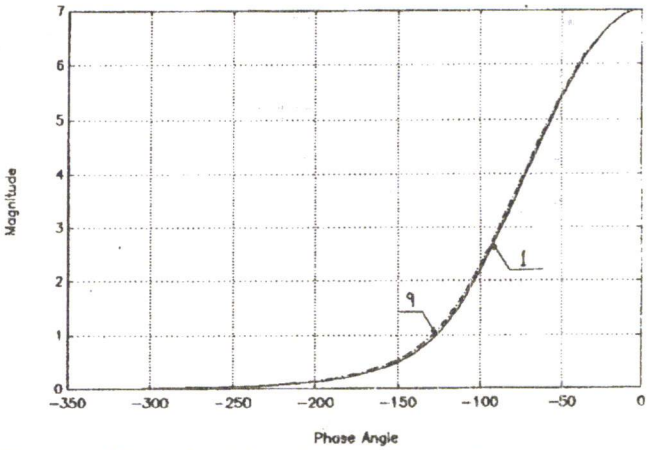

Figure 22. O.L. Magnitude-phase plots m.p.s. =6, λ=1.15, η_{vol}=0.92.

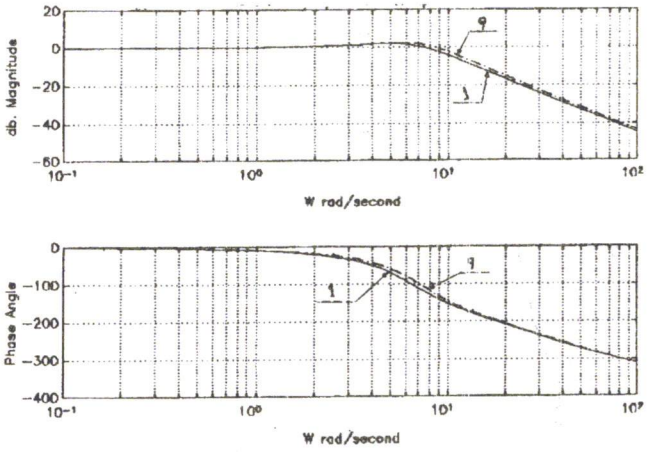

Figure 23a. C.L. Bode plots with (PD) governor$_p$=4,k_d=1s cases 1 & 9.

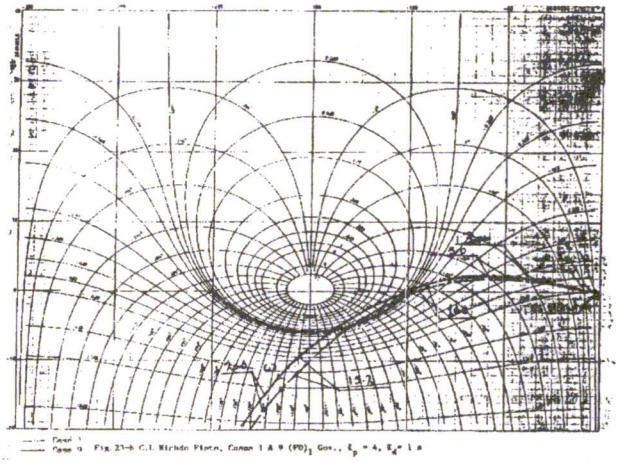

Figure 23b. C.L. Nichds plots, cases 1 & 9 $(PD)_1$ gov., k_p =4, k_d=1 s.

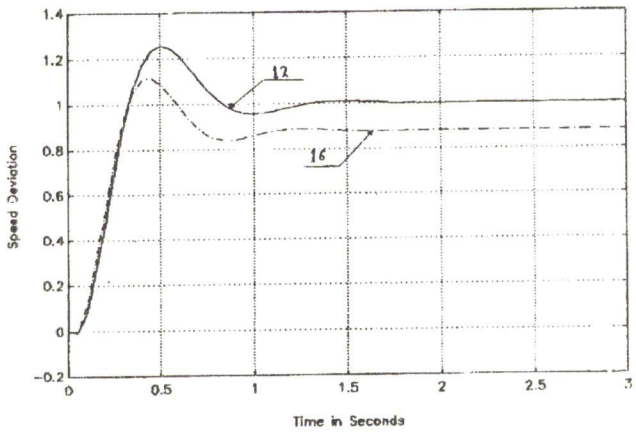

Figure 24. Transient response: λ=1.35, η_{vol}=0.95, b.m.p=12.

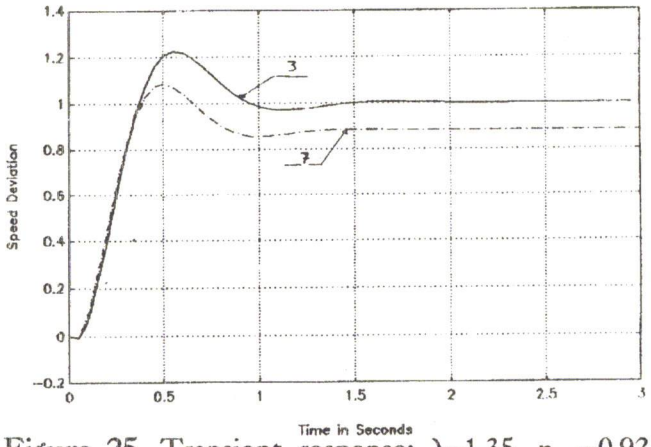

Figure 25. Transient response: λ=1.35, η_{vol}=0.92, b.m.p=10.

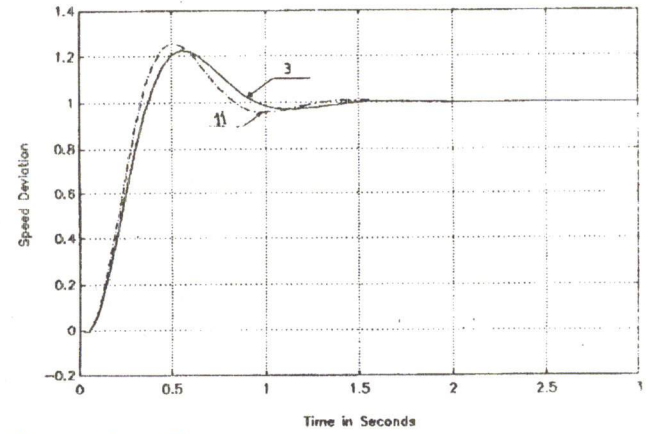

Figure 26. Transient response: λ=1.35, η_{vol}=0.92, m.p.s=6.

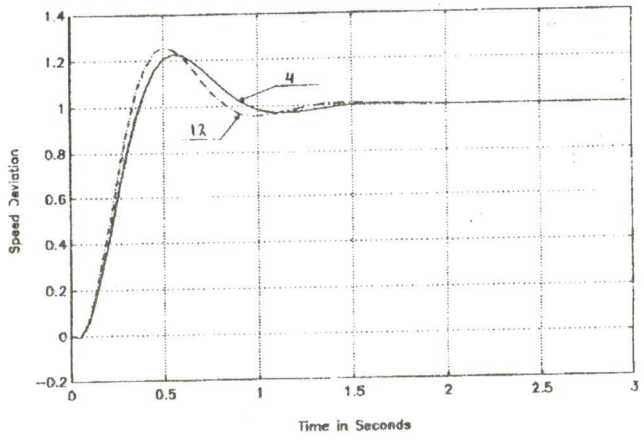

Figure 27. Transient response: λ =1.35, η_{vol}=0.95, m.p.s. =6.

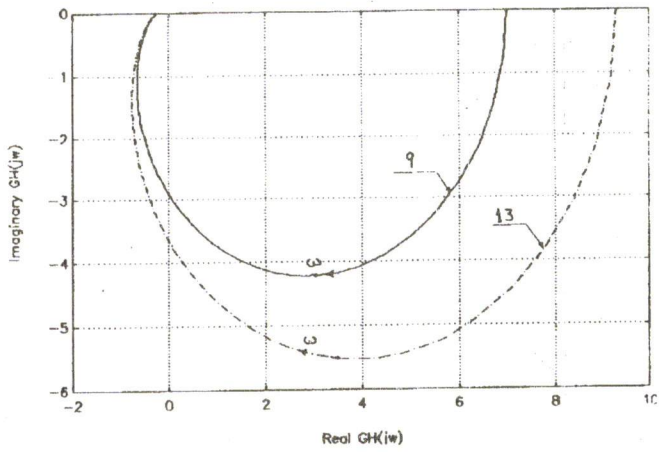

Figure 28. Polar plot b.m.e.p. =12 λ=1.15, η_{vol}=0.92.

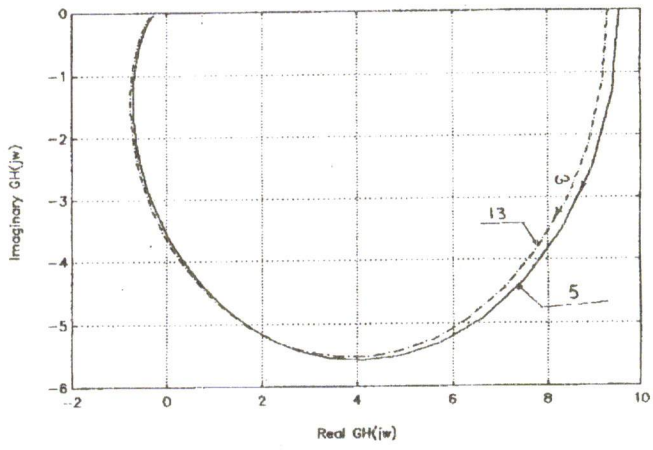

Figure 29. Polar plot m.p.s. =7, λ=1.15, η_{vol}=0.92.

DISCUSSION

In what concerns the uncontrolled plant-figures (6,11,15 and 20)- it is self-regulating, however, it is characterized by a high response e.g. 1% change in Δu corresponds to (65%-75%) change in Δn. The influence of dead and delay times is obvious in the transient responses. The effect of changing the volumetric efficiency or the excess air factor is found to be negligible, while the effect of mean piston speed or the brake mean effective pressure is proven to be more evident. An increase in the mean piston speed from /6-7/m/s -i.e. 16.6%- produces an average increase in the transient response by 6.4% On the other hand an increase in the mean effective pressure from 10-12 atm -i.e. 20%-results in an average increase in the response by about 6.6% In regards to the closed loop transient responses - figures (8,12,16,21,24,25,26 an 27)- it could be seen that the effect of changing the volumetric efficiency or the excess air factor is unnoticeable. On the contrary, the increase of the mean piston speed increases slightly the response in the neighborhood of the starting of the transients, then the phenomenon is reversed, The augmentation of mean piston speed decreases both the peak time and the maximum overshoot (M_p) and increases the static error - due to the imposed condition that case (1) is considered as the reference case. The variation in mean piston speed accompanied by a change in excess air factor does not alter the response. Similarly, the effect of mean piston speed is dominating the effect of mean effective pressure. Even-though, a change in the mean piston speed associated with changes in brake mean effective pressure, volumetric efficiency and excess air factor, dose not reshape the closed loop transient responses. As stated in the aforementioned paragraph, the influence of changing the mean effective pressure is not so strong as the effect of mean piston speed. The responses confirm that the transients of mean piston speed are apparently fortified than those of the mean effective pressure. An increase of mean effective pressure from 10-12 atm. Increases both the speed of response, the maximum overshoot(M_p) and decreases the peak time. The effect of the settling time and static error is not tangible. The influence of a change in the excess air factor or the volumetric efficiency add to the change in mean effective pressure is almost invariant and inutile. Open loop frequency responses represented in polar, Bode, Nichols, Nyquist, and decibel magnitude versus phase angle plots are displayed in figures (9,13,17,18-a.18-b,22,28 and 29). The relative stability measures namely the gain and phase margins, the phase and gain cross over frequencies are indicated in tabular form in Table (3).

The table reveals that an increase in the volumetric efficiency slightly increases the gain and phase margins,increases (ω_π) and decreases (ω_1).In resemblance with the volumetric efficiency, an increase in the excess air factor has an identical effect.On the other hand, an increase in the main piston speed decrease the gain and phase margins whereas increases the phase and gain cross over frequencies. Likewise, there exists a similarity between the influence of the increase in main piston speed and the increase in mean effective pressure on the relative stability measures.

The closed loop frequency responses are presented in Bode plots and Nichols charts in figures (10,14,19,23-a and 23-b).

No evident variation in Bode plots is observed for changes in volumetric efficiency or excess air factor. In contrast to this, minute, similar changes can be registered for changes in mean piston speed or mean effective pressure on both decibel magnitude and phase angle plots. All closed loop Bode plots are distinguished with a large bandwidth, very small resonant peak (M_r) which is located approximately at a frequency ω_1=6 (rad/s).

CONCLUSION

A simplified mathematical model for directly-coupled naturally aspirated marine Diesel engine with proportional plus derivative speed governor is derived. The engine is assumed to run at varying operating conditions. Scanned engine parameters were chosen as mean piston speed, brake mean effective pressure, volumetric efficiency and excess air factor brake mean effective pressure, volumetric efficiency and excess air factor where other steady-state engine performance characteristics vary accordingly. The unregulated plant together with automatic open and closed loops are analyzed on

digital computers in both time and frequency domains. Results obtained, emphasize that the plant alone is self regulating with excessive transient responses and the absolute stability for the feedback system is guaranteed. The effect of the mean piston speed overweighs that of the brake mean effective pressure, whereas the influences of volumetric efficiency and excess air factor on the closed loop are extremely small. An increase of mean piston speed decreases both the peak time and the maximum overshot. The response, increases the maximum overshot and decreases the peak time. Regarding the relative stability, an increase in the mean piston speed decreases both the gain and phase margins, meanwhile it increases both the phase and gain crossover frequencies. The same phenomenon is picked up for the variation of the brake mean effective pressure. A large bandwidth with very small resonant peak characterizes the closed loop Bode plots.

REFERENCES

[1] M. Mosleh and M. Hanafi, "*Part Load Dynamic Performance of Marine Diesel Engines* - Part I: *Simulation of the Propulsive Plant*", Alexandria Engineering Journal (AEJ), July 1995.

[2] M. Mosleh and M. Hanafi, "*Part Load Dynamic Performance of Marine Diesel Engines* - Part II: *Computational Assessment*", Alexandria Engineering Journal (AEJ), July 1995.

[3] M. Hanafi and A.M. El-Iraki, "*Optimized-Parameter Versus Optimal Controllers For Marine Diesel Engines*",Alexandria Engineering Journal (AEJ), July 1995.

[4] A.M. El-Iraki and M. Hanafi, "*Investigation on Non-Conventional PMD Control*",Alexandria Engineering Journal (AEJ), July 1995.

[5] R. Friedrich, "*Simulation des Regelungstechnischen Verhaltens Von Dieselmotoren auf Schiffen*", Schiffbau Forschung 28/3/1989.

[6] D. Garvey, "*Analytic Represention of Mechanical-Hydraulic and Electro-Hydraulic Governors*", Woodward Governor Company, PMCC 74-14A, U.S.A.

[7] C. Chen, "*Elements of Control Systems Analysis-Classical and Modern Approaches*", PP (298-301) Prentice-Hall, New Jersy, U.S.A., 1969.

[8] K. Ogata, "*Stat Space Analysis of Control Systems*", Perntice-Hall, Inc., N.J., U.S.A., 1967.

[9] F. Csáke, "*Modern Control Theories*", Akademiai Kiado, Budapest, 1972.

[10] F. Csáke, "*State Space Methods for Control Systems*", Akademiai Kiado, Budapest, 1977.

[11] C. Chen and L.S. Shieh, "*A Note on Expanding,PA+AP= -Q*", IEEE Trance. on automatic Control, PP. 410-420, 1967.

[12] -----, "*DERIVE 2.08, a Mathematical Assistant*", Software house Inc., U.S.A., 1990.

[13] -----, "*MATLAB 4.0, for Windows*", The Mathworks Inc., Stanford, U.S.A., 1993.